BNL-NCS-50503
(ENDF-232)

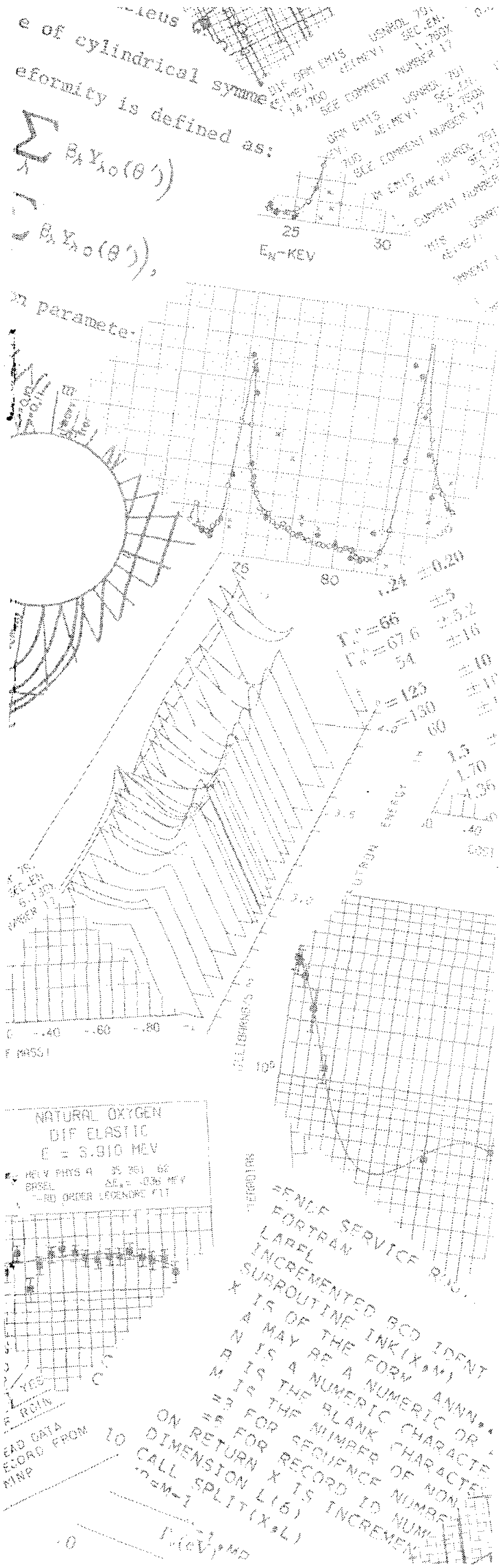

EVALUATION OF NEUTRON CROSS SECTIONS FOR THE KRYPTON ISOTOPES

A. PRINCE

August 1974

INFORMATION ANALYSIS CENTER REPORT

NATIONAL NEUTRON CROSS SECTION CENTER
BROOKHAVEN NATIONAL LABORATORY
UPTON, NEW YORK 11973

national
neutron
Cross
Section
Center

BNL-NCS-50503
(ENDF-232)
(Physics, Nuclear - TID-4500)

EVALUATION OF NEUTRON CROSS SECTIONS FOR THE KRYPTON ISOTOPES

A. PRINCE

August 1974

NATIONAL NEUTRON CROSS SECTION CENTER

BROOKHAVEN NATIONAL LABORATORY
ASSOCIATED UNIVERSITIES, INC.
UNDER CONTRACT NO. E(30-1)-16 WITH THE
UNITED STATES ENERGY RESEARCH AND DEVELOPMENT ADMINISTRATION

Printed in the United States of America
Available from
National Technical Information Service
U.S. Department of Commerce
5285 Port Royal Road
Springfield, VA 22161
Price: Domestic $5.50; Foreign $8.00;
Microfiche $2.25

March 1976 600 copies

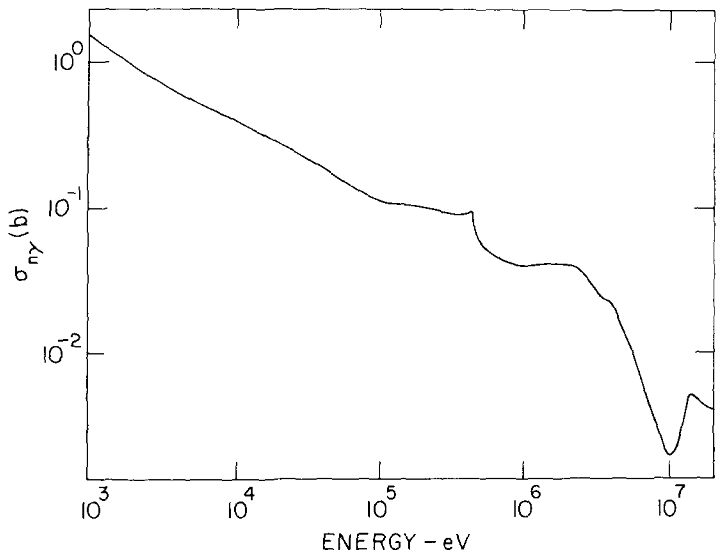

Figure 35. Capture neutron cross section for ^{78}Kr (1 keV to 20 MeV).

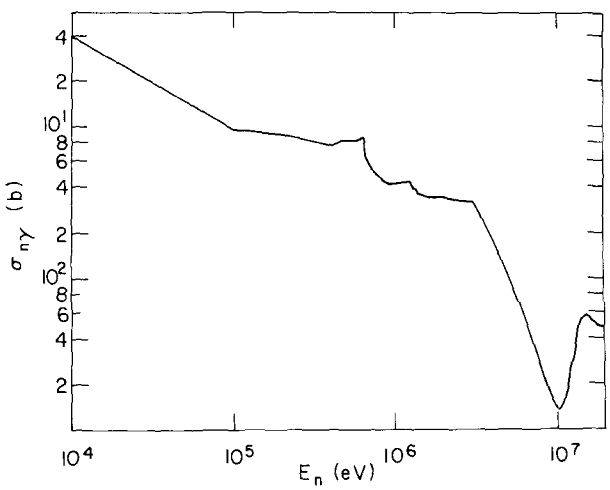

Figure 36. Capture neutron cross section for ^{80}Kr (10 keV to 20 MeV).

List of Tables

Table No.		Page
1	Experimental Resonance Parameters	15
2	Adopted Resonance Parameters	16
3	Q Values for ^{78}Kr	17
4	Q Values for ^{80}Kr	18
5	Q Values for ^{82}Kr	19
6	Q Values for ^{83}Kr	20
7	Q Values for ^{84}Kr	21
8	Q Values for ^{86}Kr	22
9	Data for Statistical Model Calculations of ^{78}Kr	23
10	Data for Statistical Model Calculations of ^{80}Kr	23
11	Data for Statistical Model Calculations of ^{82}Kr	24
12	Data for Statistical Model Calculations of ^{83}Kr	25
13	Data for Statistical Model Calculations of ^{84}Kr	26
14	Data for Statistical Model Calculations of ^{86}Kr	27
15	Neutron Activation Cross Sections at 14.4 ± 0.3 MeV for Kr Isotopes	28

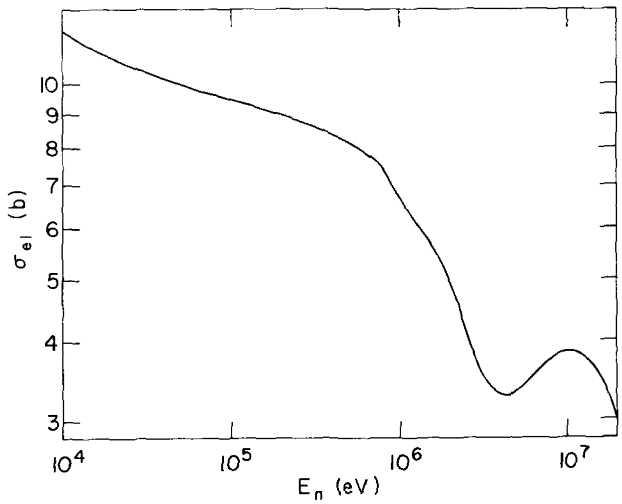

Figure 31. Elastic neutron cross section for ^{82}Kr (10 keV to 20 MeV).

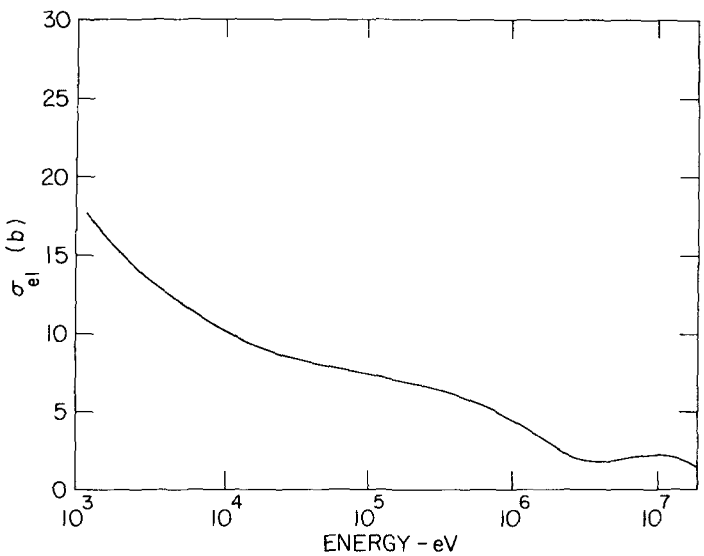

Figure 32. Elastic neutron cross section for ^{83}Kr (1.127 keV to 20 MeV).

Fig.		Page
13	Elastic Neutron Cross Section for ^{83}Kr (10^{-2} eV to 1.127 keV)	35
14	Capture Neutron Cross Section for ^{83}Kr (10^{-2} eV to 1.127 keV)	35
15	Total Neutron Cross Section for ^{84}Kr (10^{-2} eV to 2 keV)	36
16	Elastic Neutron Cross Section for ^{84}Kr (10^{-2} to 2 keV)	36
17	Capture Neutron Cross Section for ^{84}Kr (10^{-2} eV to 2 keV)	37
18	Total Neutron Cross Section for ^{86}Kr (10^{-2} eV to 10 keV)	37
19	Elastic Neutron Cross Section for ^{86}Kr (10^{-2} eV to 10 keV)	38
20	Capture Neutron Cross Section for ^{86}Kr (10^{-2} eV to 10 keV)	38
21	Total Neutron Cross Section for ^{78}Kr (1 keV to 20 MeV)	39
22	Total Neutron Cross Section for ^{80}Kr (10 keV to 20 MeV)	39
23	Total Neutron Cross Section for ^{82}Kr (10 keV to 20 MeV)	40
24	Total Neutron Cross Section for ^{83}Kr (1.127 keV to 20 MeV)	40

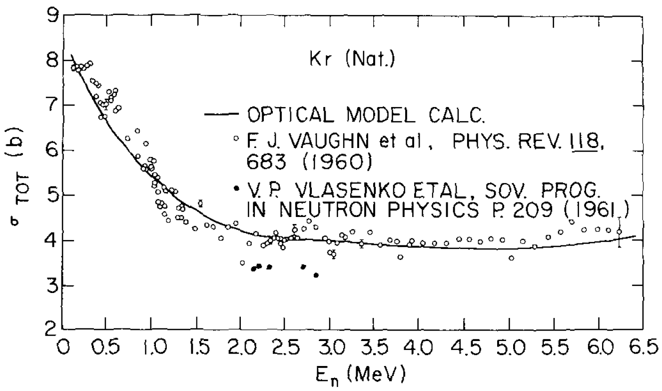

Figure 27. Optical model calc. for Kr (Nat.) (E ≤ 6.5 MeV).

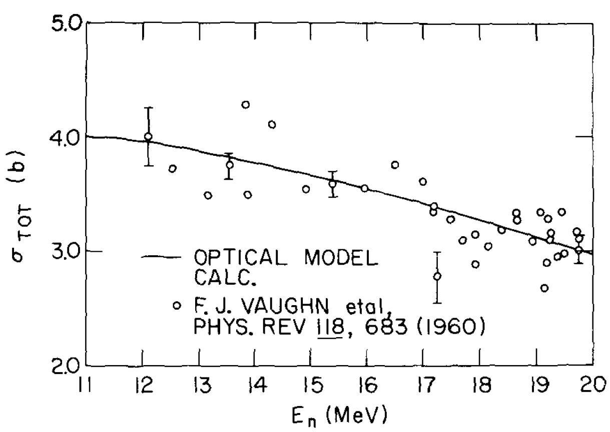

Figure 28. Optical model calc. for Kr (Nat.) (E = 11 to 20 MeV).

Fig.		Page
37	Capture Neutron Cross Section for ^{82}Kr (10 keV to 20 MeV)	47
38	Capture Neutron Cross Section for ^{83}Kr (1.127 keV to 20 MeV)	47
39	Capture Neutron Cross Section for ^{84}Kr (2 keV to 20 MeV)	48
40	Capture Neutron Cross Section for ^{86}Kr (10 keV to 20 MeV)	48

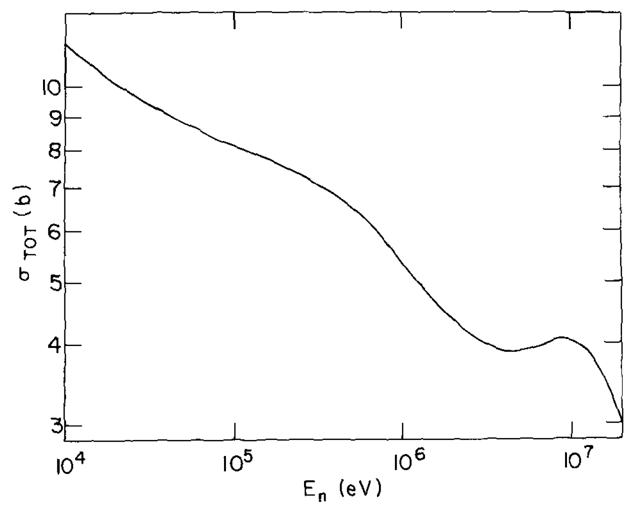

Figure 23. Total neutron cross section for ^{82}Kr (10 keV to 20 MeV).

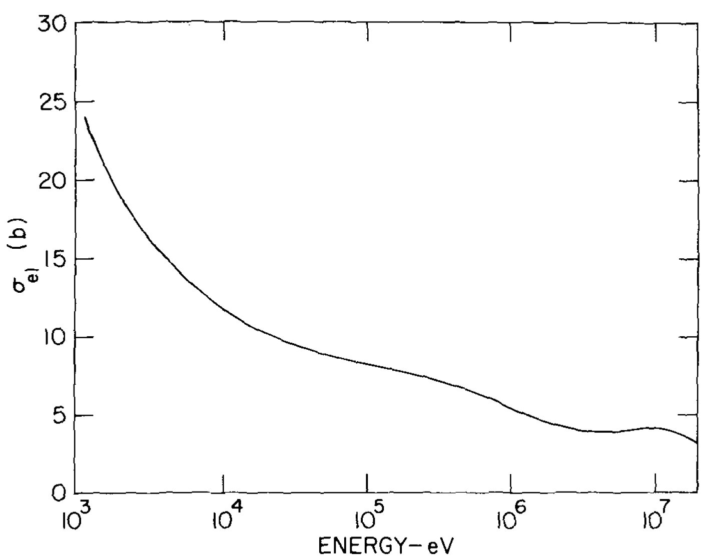

Figure 24. Total neutron cross section for ^{83}Kr (1.127 keV to 20 MeV).

Elastic Scattering

$$\sigma_{nn}^{\ell}(m) = (2\ell + 1)\,\frac{4\pi}{k_m^{\,2}}\,\sin^2 \phi_\ell$$

$$+ \frac{\pi}{k_m^{\,2}} \sum_J g_J \sum_{r=1}^{N_{res}(\ell,J)} \frac{\Gamma_{nr}^2 \cos 2\phi - 2\Gamma_{nr}\,(\Gamma_{\gamma r} + \Gamma_{fr})\,\sin^2\phi_\ell}{(E - E_r{}')^2 + \left(\frac{\Gamma_r}{2}\right)^2}$$

$$+ \frac{2(E - E_r{}')\,\Gamma_{nr}\,\sin 2\phi_\ell}{(E - E_r{}')^2 + {\frac{\Gamma_r}{2}}^2} \qquad (1)$$

Capture

$$\sigma_{n\gamma}^{\ell}(m) = \frac{\pi}{k_m^{\,2}} \sum_J g_J \sum_{r=1}^{N_{res}(\ell,J)} \frac{\Gamma_{nr}\Gamma_{\gamma r}}{(E - E_r{}')^2 + \left(\frac{\Gamma_r}{2}\right)^2} \quad . \quad (2)$$

where m is the m^{th} isotope,

$N_{res}(\ell,J)$ are the number of resonances for a given ℓ and J,

$$\Gamma_{nr}(E) = \frac{P_\ell(E)\,\Gamma_{nr}(|E_r|)}{P_\ell(|E_r|)} \quad .$$

$$\Gamma_r = \Gamma_{nr}(E) + \Gamma_{\gamma r}$$

$$E_r{}' = E_r + \left(\frac{S_\ell(|E_r|) - S_\ell(E)}{2P_\ell(E_r|)}\right)\Gamma_{nr}(|E_r|) \qquad (E \text{ in eV}) \ ,$$

$$k_m = 2.196771 \times 10^{-3} \left(\frac{AWR}{AWR + 1.0}\right) \sqrt{E}\,(eV) \quad (barns)^{-1/2} \ ,$$

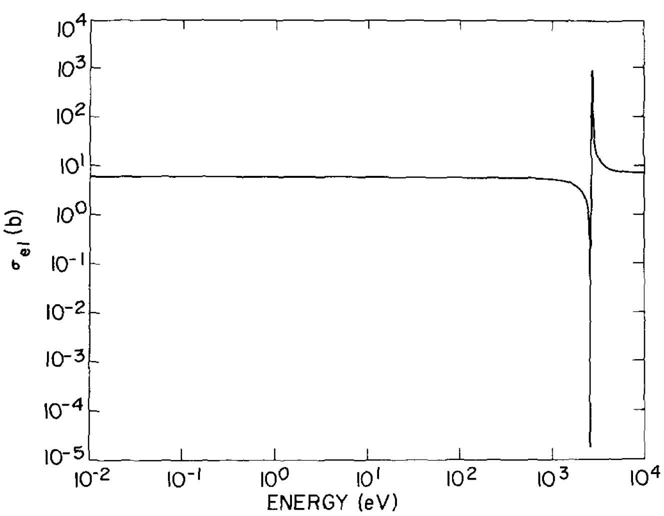

Figure 19. Elastic neutron cross section for ^{86}Kr (10^{-2} eV to 10 keV).

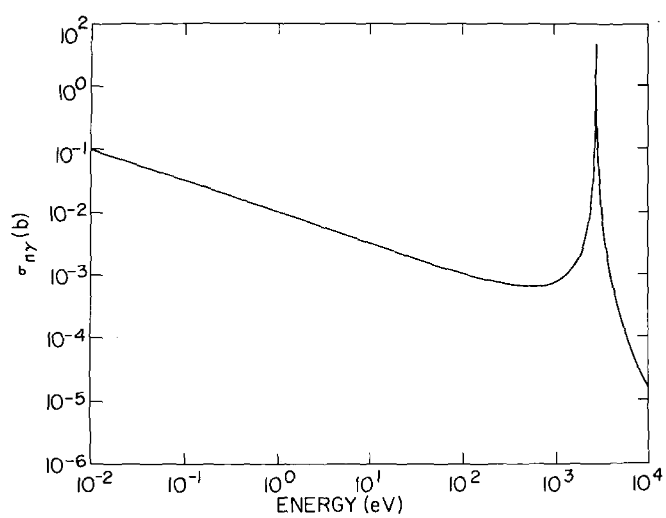

Figure 20. Capture neutron cross section for ^{86}Kr (10^{-2} eV to 10 keV).

where

A = mass of nucleus

U = effective energy of excitation ($U = E_B - \Delta$)

E_B = binding energy of compound nucleus

$\Delta = \delta(N) + \delta(p)$ the pairing energy

I = spin of target nucleus

a = single-particle state density parameter near the Fermi surface.

The relation between a and A are based on the analysis of Cook et al.[6] where

$\frac{a}{A} = 0.009175 + 0.142$

$S = S(N) + S(a)$ shell correction parameter

Eq. (1) produced the following radiation widths

Kr 78	Γ_γ = 266 meV
Kr 80	Γ_γ = 237 meV
Kr 82	Γ_γ = 236 meV
Kr 83	Γ_γ = 233 meV
Kr 84	Γ_γ = 226 meV
Kr 86	Γ_γ = 168 meV

A comparison of these widths with experimental data and calculations of Malecky et al.[5] are shown in Figure (1).

Krypton-78 (MAT 1181)

For Kr^{78} the experimental data in Table 1 yielded a value of $\sigma_{n\gamma}$(2200m) = 0.156b which is much lower than the value of 4.71 ± 0.68b[7].

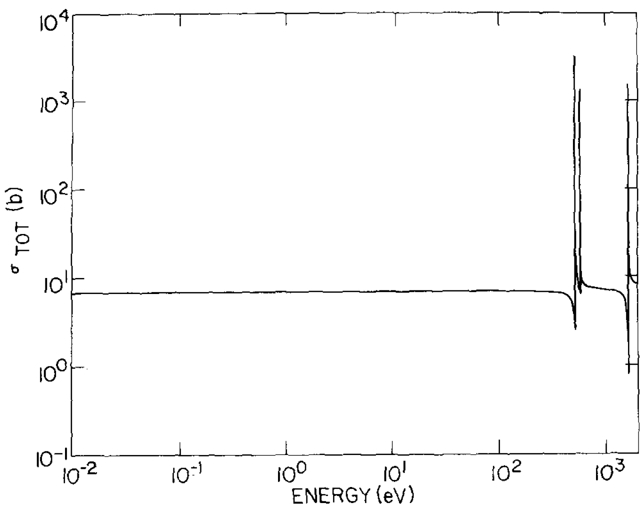

Figure 15. Total neutron cross section for ^{84}Kr (10^{-2} eV to 2 keV).

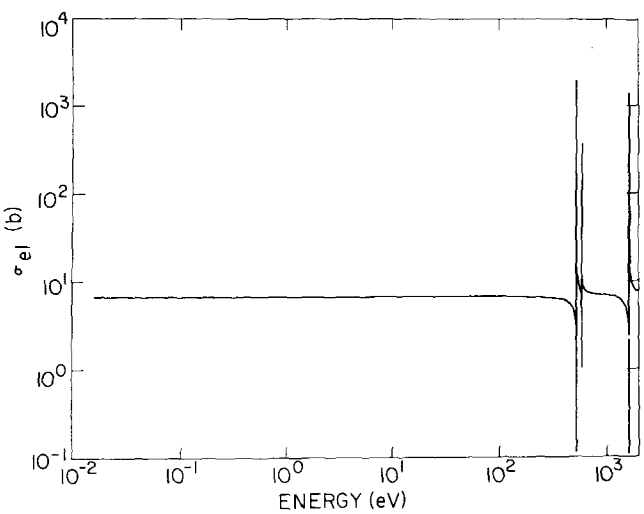

Figure 16. Elastic neutron cross section for ^{84}Kr (10^{-2} eV to 2 keV).

<u>Krypton-80 (MAT 1182)</u>

The experimental values of the 2200 m/s absorption cross section is reported as 11.3 ± 4b[12], $\sigma_{n\gamma}^{m+g}$ = 14.0 ± 1.5b,[11] σ_{γ}^{m} = 4.55 ± 0.65[7,11]; and 15.6 ± 1.9b[13]

Using the resonance parameters shown in Table 2, where a bound level at 57.21 ev has been assumed, produced a calculated value of 14.31b which is well within the quoted experimental values.

The potential scattering cross section was taken to be the same as that used for ^{78}Kr (σ_{pot} = 6.2b). The resonance integral was established using the parameter in Table 2 which produced a value of 59.3b ($E_{cut-off}$ = 0.5 eV). This calculated value compares favorably with the experimental value of I_{γ} = 56.1 ± 2.8[12] and the recommended I_{γ} = 56.1 ± 5.6b.[11] The total, elastic and capture cross sections generated from the resonance data in Table 2 are given in Figures 6 - 8.

<u>Krypton-82 (MAT 1183)</u>

In addition to the reported resonance at 39.8 ev (Table 1) along with the resonance parameters given in Table 2 it has necessary to assume a bound level at -42.83 ev (Table 2) to yield a thermal capture cross section of $\sigma_{n\gamma}$ = 30.20 b. An experimental value leading to the metastable state in ^{83}Kr of $\sigma_{n\gamma}^{m}$ = 20.0 ± 3.5 b has been reported by Reference 7. The value calculated here is barely within the recommended value of $\sigma_{n\gamma}^{m+g}$ = 45 ± 15 b.[11] A value $\sigma_{n\gamma}$ = 25.0 b has been estimated by Reference 14. As with

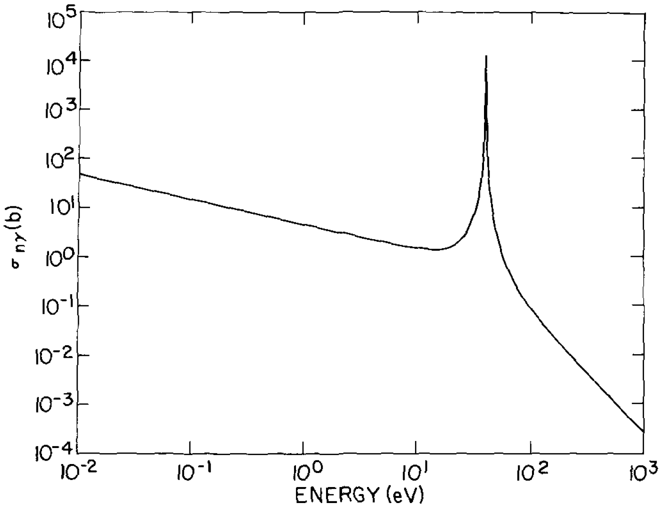

Figure 11. Capture neutron cross section for ^{82}Kr (10^{-2} eV to 1 keV).

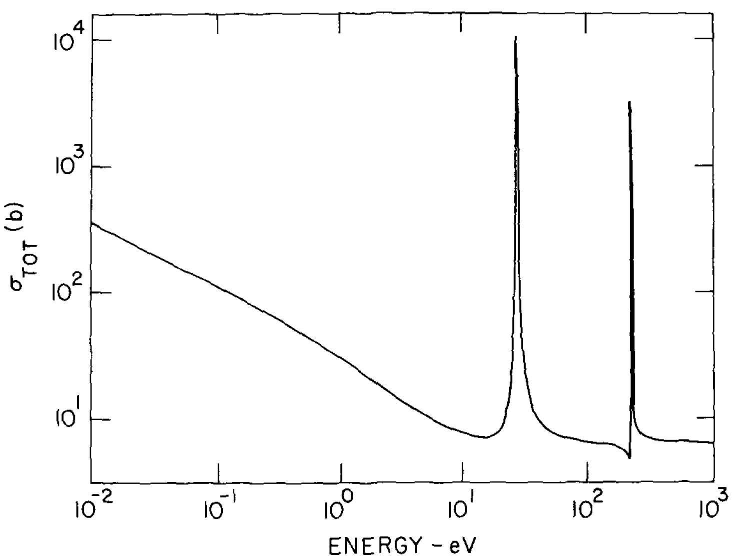

Figure 12. Total neutron cross section for ^{83}Kr (10^{-2} eV to 1.127 keV).

Krypton 84 (MAT 1185)

The unassigned resonance in Figure 2 was assumed to be due to ^{89}Kr at an energy of 1625.0 eV, with a neutron width Γ_n = 2.184.0 eV and Γ_γ = 226.0 eV. This resonance along with the other two lower lying resonances at 519.0 and 580.0 eV yielded a thermal capture cross section $\sigma_{n\gamma}$ (0.0253 ev) = 0.0864 b. An experimental value for the 4.4 hr. ^{85}Kr was reported by Kondaiah et al. to be equal to 0.09 ± 0.013 b, and a value of 0.042 ± 0.004 b to the 10.74 yr. ^{85}Kr. Reference 11 gives a recommended value of $\sigma_{n\gamma}$ = 0.130 ± 0.014 b [$^{85}Kr^{m+g}$], while Reference 17 reports $\sigma_{n\gamma}$ = 0.16 b. The potential scattering cross section remains the same as for the other Kr isotopes.

A calculated resonance integral of magnitude 3.27 b is in good agreement with the calculated value of 2.7 ± 0.7 b reported in Reference 11, and excellent agreement with I_γ = 3.54.(17)

The total, elastic or capture cross sections in the energy range 10^{-2} eV to 1.133 keV are presented in Figures 15 - 17.

Krypton-86 (MAT 1186)

No resonance parameters have been experimentally determined for ^{86}Kr, therefore, it was necessary to make certain assumptions. From Figure 2 there is an unassigned resonance at an energy of approximately 2700 eV.

Since the thermal capture cross section and resonance integral for ^{86}Kr has been estimated to be very small (see following references) this resonance was taken to be due to this isotope.

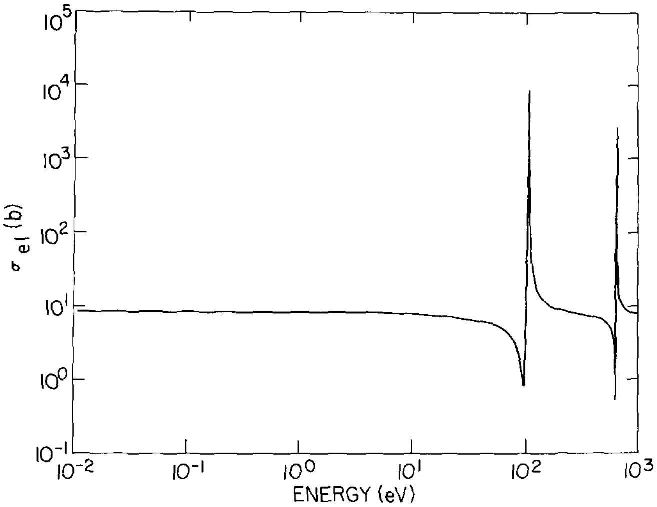

Figure 7. Elastic neutron cross section for ^{80}Kr (10^{-2} eV to 1 keV).

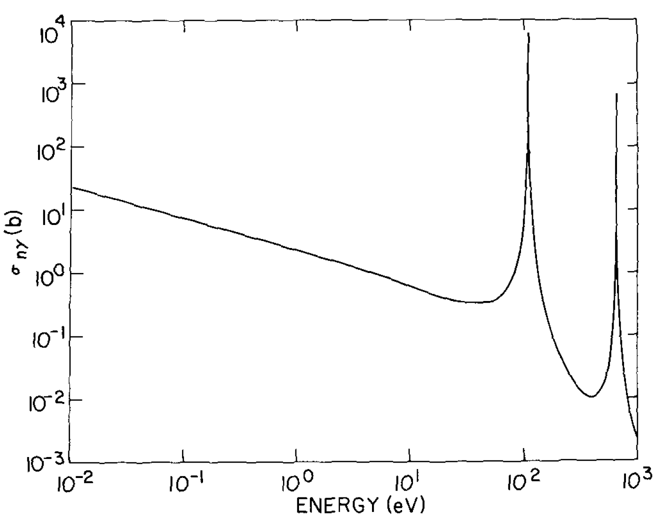

Figure 8. Capture neutron cross section for ^{80}Kr (10^{-2} eV to 1 keV).

3.1 Optical Model Calculations

The optical potential was the usual combination Saxon-Woods with real $V(r)$, imaginary $W(r)$ and spin-orbit $V_{SO}(r)$ parts, given by

$$V(r) = V_R f(r, R_R, \alpha_R) \qquad \text{central real}$$

$$+ V_{SO}\sigma\cdot\ell\lambda\!\!\!^{-}\pi^2 (1/r)(d/dr)[f(r, R_{SO}, a_{SO})] \qquad \text{spin-orbit}$$

and

$$W(r) = -W_V f(r, R_I', \alpha_I'), \qquad \text{imaginary volume}$$

$$+W_{SF} 4a_I (d/dr)[f(r, R_I, a_I)] , \qquad \text{imaginary surface,}$$

where

$$f(r, R, \alpha) = [1 + \exp (r - R)/a]^{-1} .$$

$$R_R = r_R A^{1/3} ,$$

$$R_{SO} = r_{SO} A^{1/3} ,$$

$$R_I' = r_I' A^{1/3} ,$$

$$R_I = r_I A^{1/3} .$$

The strengths of the various parameters in the above equations were taken from the work of Becchetti and Greenlees (22) where an isospin and energy dependence in the potentials has been considered.

$$V_R = 56.3 - 0.32E - 24.0 (N - Z)/A ,$$

$$r_R = 1.17, \qquad a_R = 0.75 ,$$

W_V = 0.22E - 1.56 or zero whichever is greater,*

$$W_{SF} = 13.0 - 0.25E - 12.0 (N - Z)/A$$

or zero, whichever is greater,

$$r_I = r_I' = 1.26, \qquad a_I = a_I' = 0.58 ,$$

*The volume imaginary $W_V = 0$ for this evaluation.

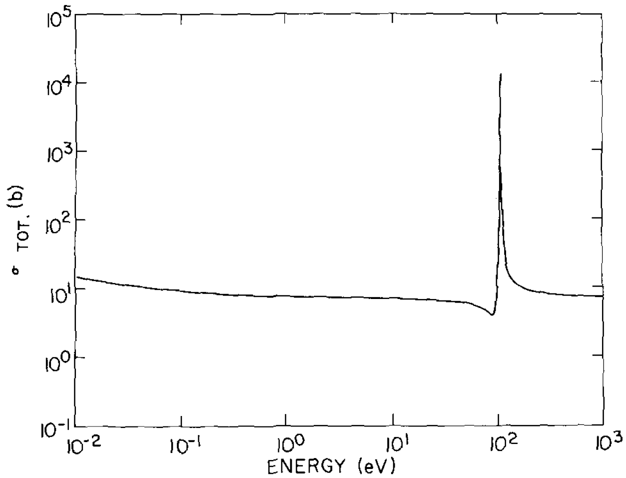

Figure 3. Total neutron cross section for ^{78}Kr (10^{-2} eV to 1 keV).

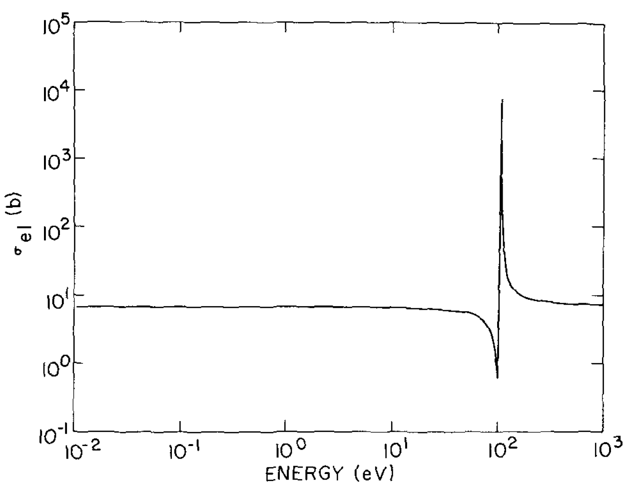

Figure 4. Elastic neutron cross section for ^{78}Kr (10^{-2} eV to 1 keV).

shows a comparison of these calculations with the experimental results of Kondaiah et al.[25]

4.0 Angular Distribution of Secondary Neutrons

The angular distribution of the elastically scattered neutrons was interpreted in terms of a Legendre polynomial fit using CHAD[26] for File 4.

For the inelastically scattered neutrons and the n-2n reactions the distribution was assumed to be isotropic.

5.0 Energy Distribution of Secondary Neutrons

The energy distributions of neutrons due to the n-2n, n-3n and continuum inelastic scattering were expressed in terms of a normalized probability distribution having an evaporation spectrum given by

$$f(E \rightarrow E') = \frac{E'}{I} e^{-E'/\theta}$$

I = normalization constant

θ = nuclear temperature

The energy dependence of θ was formulated according to Gilbert and Cameron.[27]

Table 15

Neutron Activation Cross Sections at 14.4 ± 0.3 MeV for Kr Isotopes

Reaction	Half-Life	Measured cross section (mb) Ref. 25	ENDF (mb) This Work
$^{78}Kr(n,2n)^{77}Kr$	1.19 h	245 ± 20	245.2
$^{80}Kr(n,2n)^{79(m+g)}Kr$	34.92 h	810 ± 60	890.0
$^{80}Kr(n,2n)^{79m}Kr$	55 sec	415 ± 50	
$^{82}Kr(n,2n)^{81m}Kr$	13 sec	160 ± 15	
$^{86}Kr(n,2n)^{85m}Kr$	4.4 h	350 ± 35	
$^{80}Kr(n,p)^{80m}Br$	4.3 h	55 ± 9	
$^{82}Kr(n,p)^{82(m+g)}Br$	35.34 h	23 ± 4	20.5
$^{84}Kr(n,p)^{84}Br$	31.8 min	8.5 ± 1.5	9.4
$^{86}Kr(n,\alpha)^{83g}Se$	22.6 min	1.2 ± 0.2	1.49

24. V. Benzi, CCON-NW/10.

25. E. Kondaiah et al., Nucl. Phys. A120, 337 (1968).

26. R.F. Berland, CHAD, NAA-SR-11231.

27. A. Gilbert and A.G.W. Cameron, Can. J. Phys. 43, 1446 (1965).

Table 14

Data for Statistical Model Calculations of ^{86}Kr

Level Scheme	
E(MeV)	J^{π}
0.0	0^+
0.95	2^+
1.57	2^+
2.76	0^+
$\frac{\langle \Gamma_\gamma \rangle}{\langle D \rangle}$	7.0×10^{-6}
$E_{cut-off}$	2.8 MeV

Table 2

Adopted Resonance Parameters

E_R	Γ_T (mV)	Γ_n (mV)	Γ_γ (mV)
^{78}Kr (MAT 1181)			
-137.0	634.0	368.0	266.0
106.0	573.0	307.0	266.0
^{80}Kr (MAT 1182)			
- 57.21	519.0	282.0	237.0
106.0	573.0	336.0	237.0
640.0	1237.0	1000.0	237.0
^{82}Kr (MAT 1183)			
- 42.83	496.0	260.0	236.0
39.80	324.3	88.3	236.0
^{83}Kr (MAT 1184)			
- 3.90	245.44	12.44	233.0
27.9	300.0	67.0	233.0
233.0	523.0	290.0	233.0
^{84}Kr (MAT 1185)			
519.0	571.0	345.0	226.0
580.0	313.0	87.0	226.0
1625.0	2410.0	2184.0	226.0
^{86}Kr (MAT 1186)			
2730.0	3568.0	3400.0	168.0

Table 11

Data for Statistical Model Calculations of ^{82}Kr

Level Scheme

E(MeV)	J^{π}
0.0	0^+
0.777	2^+
1.4750	2^+
1.8200	4^+
1.9550	2^+
2.0950	4^+
2.190	0^+
2.426	3^+
2.555	2^+
2.648	4^-
2.828	5^-
$\frac{\langle \Gamma_\gamma \rangle}{\langle D \rangle}$	3.34×10^{-4}
$E_{cut\text{-}off}$	2.9 MeV

Table 4

Q Values for ^{80}Kr

Reaction	-Q(MeV)	ENDF MT
(n,p)	1.228	103
(n,He^3)	7.730	106
(n,n'd)	17.581	
$(n,n'He^4)$	5.066	22
(n,He^4n')	5.066	22
(n,p,He^4)	7.252	
(n,2n)	11.525	16
(n,d)	6.886	104
(n,He^4)	-0.969	107
(n,n't)	19.610	
(n,p,n')	9.111	28
(n,He^4,p)	7.252	
(n,3n)	19.893	17
(n,t)	11.322	105
(n,n'p)	9.111	28
$(n,n'He^3)$	18.226	
(n,2p)	8.470	
(n,d,n')	17.581	

% Abundance = 2.27

Mass = 79,916376

Binding energy of last neutron in compound nucleus = 7.850

Table 8

Q Values for ^{86}Kr

Reaction	-Q(MeV)	ENDF MT
(n,p)	6.520	103
(n,He^3)	14.202	106
(n,n'd)	18.669	
(n,n'He^4)	7.511	22
(n,He^4n')	7.511	22
(n,p,He^4)	14.308	
(n,2n)	9.860	16
(n,d)	9.655	104
(n,He^4)	-1.384	107
(n,n't)	19.194	
(n,p,n')	11.880	28
(n,He^4,p)	14.208	
(n,3n)	16.971	17
(n,t)	12.410	105
(n,n'p)	11.880	28
(n,n'He^3)	22.753	
(n,2p)	17.111	
(n,d,n')	18.669	

% Abundance = 17.37

Mass = 85.910616

Binding energy of last neutron in compound nucleus = 5.511

Table 6

Q Values for ^{83}Kr

Reaction	-Q(MeV)	ENDF MT
(n,p)	0.187	103
(n,He^3)	10.461	106
(n,n'd)	15.151	
(n,n'He^4)	6.479	22
(n,He^4n')	6.479	22
(n,p,He^4)	7.942	
(n,2n)	7.467	16
(n,d)	7.548	104
(n,He^4)	-1.526	107
(n,n't)	19.052	
(n,p,n')	9.773	28
(n,He^4,p)	7.942	
(n,3n)	18.450	17
(n,t)	8.892	105
(n,n'p)	9.773	28
(n,n'He^3)	17.162	
(n,2p)	8.907	
(n,d,n')	15.151	

% Abundance = 11.55

Mass = 82.914131

Binding energy of last neutron in compound nucleus = 10.518

Table 6

Q Values for ^{83}Kr

Reaction	-Q (MeV)	ENDF MT
(n,p)	0.187	103
(n,He^3)	10.461	106
(n,n'd)	15.151	
(n,n'He^4)	6.479	22
(n,He^4n')	6.479	22
(n,p,He^4)	7.942	
(n,2n)	7.467	16
(n,d)	7.548	104
(n,He^4)	-1.526	107
(n,n't)	19.052	
(n,p,n')	9.773	28
(n,He^4,p)	7.942	
(n,3n)	18.450	17
(n,t)	8.892	105
(n,n'p)	9.773	28
(n,n'He^3)	17.162	
(n,2p)	8.907	
(n,d,n')	15.151	

% Abundance = 11.55

Mass = 82.914131

Binding energy of last neutron in compound nucleus = 10.518

Table 8

Q Values for ^{86}Kr

Reaction	-Q(MeV)	ENDF MT
(n,p)	6.520	103
(n,He^3)	14.202	106
(n,n'd)	18.669	
(n,n'He^4)	7.511	22
(n,He^4n')	7.511	22
(n,p,He^4)	14.308	
(n,2n)	9.860	16
(n,d)	9.655	104
(n,He^4)	-1.384	107
(n,n't)	19.194	
(n,p,n')	11.880	28
(n,He^4,p)	14.208	
(n,3n)	16.971	17
(n,t)	12.410	105
(n,n'p)	11.880	28
(n,n'He^3)	22.753	
(n,2p)	17.111	
(n,d,n')	18.669	

% Abundance = 17.37

Mass = 85.910616

Binding energy of last neutron in compound nucleus = 5.511

Table 4

Q Values for ^{80}Kr

Reaction	-Q(MeV)	ENDF MT
(n,p)	1.228	103
(n,He^3)	7.730	106
(n,n'd)	17.581	
(n,n'He^4)	5.066	22
(n,He^4n')	5.066	22
(n,p,He^4)	7.252	
(n,2n)	11.525	16
(n,d)	6.886	104
(n,He^4)	-0.969	107
(n,n't)	19.610	
(n,p,n')	9.111	28
(n,He^4,p)	7.252	
(n,3n)	19.893	17
(n,t)	11.322	105
(n,n'p)	9.111	28
(n,n'He^3)	18.226	
(n,2p)	8.470	
(n,d,n')	17.581	

% Abundance = 2.27

Mass = 79,916376

Binding energy of last neutron in compound nucleus = 7.850

Table 11

Data for Statistical Model Calculations of ^{82}Kr

Level Scheme

E(MeV)	J^{π}
0.0	0^+
0.777	2^+
1.4750	2^+
1.8200	4^+
1.9550	2^+
2.0950	4^+
2.190	0^+
2.426	3^+
2.555	2^+
2.648	4^-
2.828	5^-
$\frac{\langle \Gamma_\gamma \rangle}{\langle D \rangle}$	3.34×10^{-4}
$E_{cut\text{-}off}$	2.9 MeV

Table 2

Adopted Resonance Parameters

E_R	Γ_T (mV)	Γ_n (mV)	Γ_γ (mV)
^{78}Kr (MAT 1181)			
-137.0	634.0	368.0	266.0
106.0	573.0	307.0	266.0
^{80}Kr (MAT 1182)			
- 57.21	519.0	282.0	237.0
106.0	573.0	336.0	237.0
640.0	1237.0	1000.0	237.0
^{82}Kr (MAT 1183)			
- 42.83	496.0	260.0	236.0
39.80	324.3	88.3	236.0
^{83}Kr (MAT 1184)			
- 3.90	245.44	12.44	233.0
27.9	300.0	67.0	233.0
233.0	523.0	290.0	233.0
^{84}Kr (MAT 1185)			
519.0	571.0	345.0	226.0
580.0	313.0	87.0	226.0
1625.0	2410.0	2184.0	226.0
^{86}Kr (MAT 1186)			
2730.0	3568.0	3400.0	168.0

Table 14

Data for Statistical Model Calculations of ^{86}Kr

Level Scheme	
E(MeV)	J^{π}
0.0	0^+
0.95	2^+
1.57	2^+
2.76	0^+
$\frac{\langle\Gamma_\gamma\rangle}{\langle D\rangle}$	7.0×10^{-6}
$E_{cut-off}$	2.8 MeV

24. V. Benzi, CCON-NW/10.

25. E. Kondaiah et al., Nucl. Phys. A120, 337 (1968).

26. R.F. Berland, CHAD, NAA-SR-11231.

27. A. Gilbert and A.G.W. Cameron, Can. J. Phys. 43, 1446 (1965).

Table 15

Neutron Activation Cross Sections at 14.4 ± 0.3 MeV for Kr Isotopes

Reaction	Half-Life	Measured cross section (mb) Ref. 25	ENDF (mb) This Work
$^{78}Kr(n,2n)^{77}Kr$	1.19 h	245 ± 20	245.2
$^{80}Kr(n,2n)^{79(m+g)}Kr$	34.92 h	810 ± 60	890.0
$^{80}Kr(n,2n)^{79m}Kr$	55 sec	415 ± 50	
$^{82}Kr(n,2n)^{81m}Kr$	13 sec	160 ± 15	
$^{86}Kr(n,2n)^{85m}Kr$	4.4 h	350 ± 35	
$^{80}Kr(n,p)^{80m}Br$	4.3 h	55 ± 9	
$^{82}Kr(n,p)^{82(m+g)}Br$	35.34 h	23 ± 4	20.5
$^{84}Kr(n,p)^{84}Br$	31.8 min	8.5 ± 1.5	9.4
$^{86}Kr(n,\alpha)^{83g}Se$	22.6 min	1.2 ± 0.2	1.49

shows a comparison of these calculations with the experimental results of Kondaiah et al.[25]

4.0 Angular Distribution of Secondary Neutrons

The angular distribution of the elastically scattered neutrons was interpreted in terms of a Legendre polynomial fit using CHAD[26] for File 4.

For the inelastically scattered neutrons and the n-2n reactions the distribution was assumed to be isotropic.

5.0 Energy Distribution of Secondary Neutrons

The energy distributions of neutrons due to the n-2n, n-3n and continuum inelastic scattering were expressed in terms of a normalized probability distribution having an evaporation spectrum given by

$$f(E \rightarrow E') = \frac{E'}{I} e^{-E'/\theta}$$

I = normalization constant

θ = nuclear temperature

The energy dependence of θ was formulated according to Gilbert and Cameron.[27]

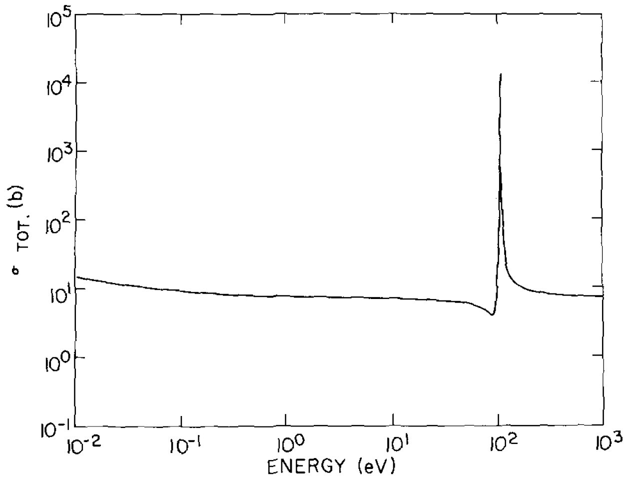

Figure 3. Total neutron cross section for ^{78}Kr (10^{-2} eV to 1 keV).

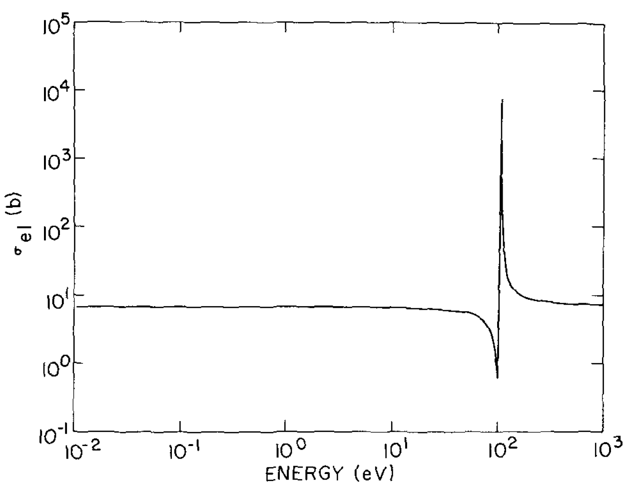

Figure 4. Elastic neutron cross section for ^{78}Kr (10^{-2} eV to 1 keV).

3.1 Optical Model Calculations

The optical potential was the usual combination Saxon-Woods with real V(r), imaginary W(r) and spin-orbit $V_{SO}(r)$ parts, given by

$$V(r) = V_R f(r, R_R, \alpha_R) \qquad \text{central real}$$

$$+ V_{SO} \sigma \cdot \ell \lambda\!\!\!^{-}\pi^2 (1/r)(d/dr)[f(r, R_{SO}, a_{SO})] \qquad \text{spin-orbit}$$

and

$$W(r) = -W_V f(r, R_I', \alpha_I'), \qquad \text{imaginary volume}$$

$$+W_{SF} 4a_I (d/dr)[f(r, R_I, a_I)] , \qquad \text{imaginary surface,}$$

where

$$f(r, R, \alpha) = [1 + \exp(r - R)/a]^{-1} .$$

$$R_R = r_R A^{1/3} ,$$

$$R_{SO} = r_{SO} A^{1/3} ,$$

$$R_I' = r_I' A^{1/3} ,$$

$$R_I = r_I A^{1/3} .$$

The strengths of the various parameters in the above equations were taken from the work of Becchetti and Greenlees[22] where an isospin and energy dependence in the potentials has been considered.

$$V_R = 56.3 - 0.32E - 24.0 (N - Z)/A ,$$

$$r_R = 1.17, \qquad a_R = 0.75 ,$$

W_V = 0.22E - 1.56 or zero whichever is greater,*

$$W_{SF} = 13.0 - 0.25E - 12.0 (N - Z)/A$$

or zero, whichever is greater,

$$r_I = r_I' = 1.26, \qquad a_I = a_I' = 0.58 ,$$

*The volume imaginary W_V = 0 for this evaluation.

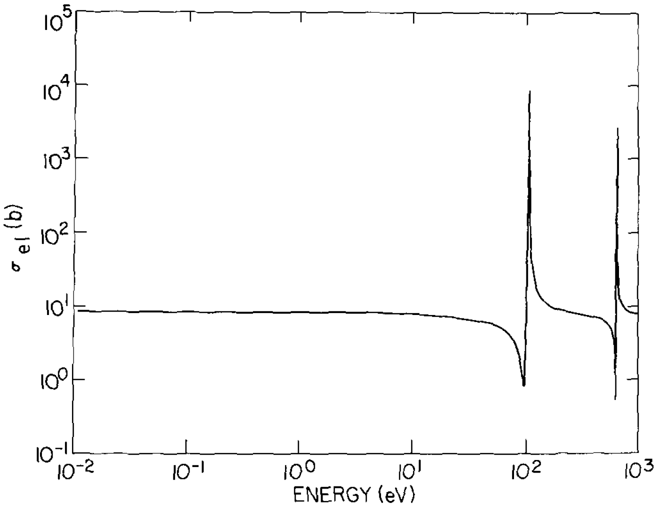

Figure 7. Elastic neutron cross section for ^{80}Kr (10^{-2} eV to 1 keV).

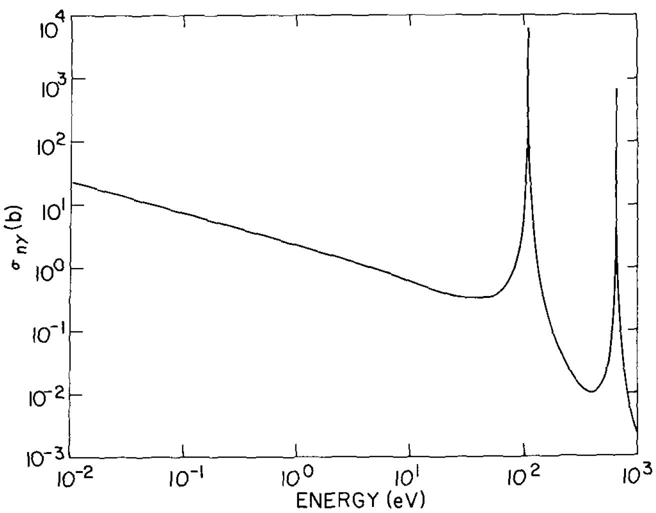

Figure 8. Capture neutron cross section for ^{80}Kr (10^{-2} eV to 1 keV).

Krypton 84 (MAT 1185)

The unassigned resonance in Figure 2 was assumed to be due to ^{89}Kr at an energy of 1625.0 eV, with a neutron width Γ_n = 2.184.0 eV and Γ_γ = 226.0 eV. This resonance along with the other two lower lying resonances at 519.0 and 580.0 eV yielded a thermal capture cross section $\sigma_{n\gamma}$ (0.0253 ev) = 0.0864 b. An experimental value for the 4.4 hr. ^{85}Kr was reported by Kondaiah et al. to be equal to 0.09 ± 0.013 b, and a value of 0.042 ± 0.004 b to the 10.74 yr. ^{85}Kr. Reference 11 gives a recommended value of $\sigma_{n\gamma}$ = 0.130 ± 0.014 b [$^{85}Kr^{m+g}$], while Reference 17 reports $\sigma_{n\gamma}$ = 0.16 b. The potential scattering cross section remains the same as for the other Kr isotopes.

A calculated resonance integral of magnitude 3.27 b is in good agreement with the calculated value of 2.7 ± 0.7 b reported in Reference 11, and excellent agreement with I_γ = 3.54.(17)

The total, elastic or capture cross sections in the energy range 10^{-2} eV to 1.133 keV are presented in Figures 15 - 17.

Krypton-86 (MAT 1186)

No resonance parameters have been experimentally determined for ^{86}Kr, therefore, it was necessary to make certain assumptions. From Figure 2 there is an unassigned resonance at an energy of approximately 2700 eV.

Since the thermal capture cross section and resonance integral for ^{86}Kr has been estimated to be very small (see following references) this resonance was taken to be due to this isotope.

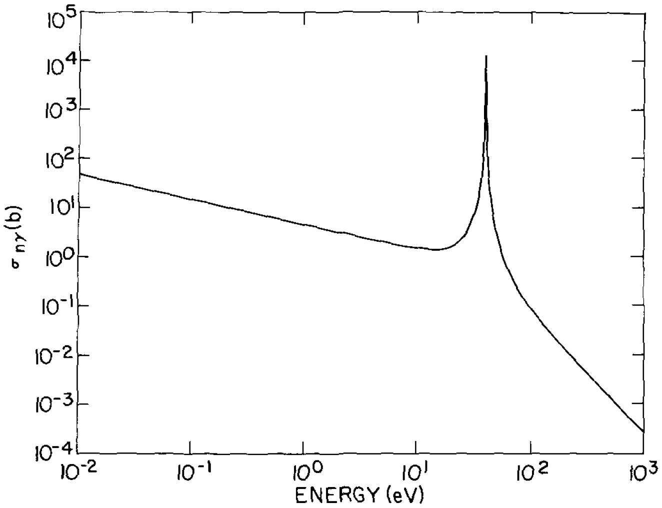

Figure 11. Capture neutron cross section for ^{82}Kr (10^{-2} eV to 1 keV).

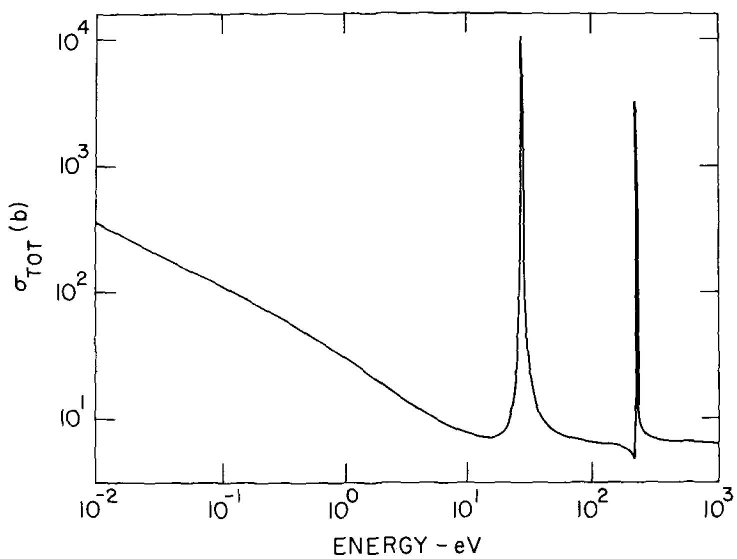

Figure 12. Total neutron cross section for ^{83}Kr (10^{-2} eV to 1.127 keV).

Krypton-80 (MAT 1182)

The experimental values of the 2200 m/s absorption cross section is reported as 11.3 ± 4b[12], $\sigma_{n\gamma}^{m+g}$ = 14.0 ± 1.5b,[11] σ_{γ}^{m} = 4.55 ± 0.65[7,11]; and 15.6 ± 1.9b[13]

Using the resonance parameters shown in Table 2, where a bound level at 57.21 ev has been assumed, produced a calculated value of 14.31b which is well within the quoted experimental values.

The potential scattering cross section was taken to be the same as that used for ^{78}Kr (σ_{pot} = 6.2b). The resonance integral was established using the parameter in Table 2 which produced a value of 59.3b ($E_{cut-off}$ = 0.5 eV). This calculated value compares favorably with the experimental value of I_{γ} = 56.1 ± 2.8[12] and the recommended I_{γ} = 56.1 ± 5.6b.[11] The total, elastic and capture cross sections generated from the resonance data in Table 2 are given in Figures 6 - 8.

Krypton-82 (MAT 1183)

In addition to the reported resonance at 39.8 ev (Table 1) along with the resonance parameters given in Table 2 it has necessary to assume a bound level at -42.83 ev (Table 2) to yield a thermal capture cross section of $\sigma_{n\gamma}$ = 30.20 b. An experimental value leading to the metastable state in ^{83}Kr of $\sigma_{n\gamma}^{m}$ = 20.0 ± 3.5 b has been reported by Reference 7. The value calculated here is barely within the recommended value of $\sigma_{n\gamma}^{m+g}$ = 45 ± 15 b.[11] A value $\sigma_{n\gamma}$ = 25.0 b has been estimated by Reference 14. As with

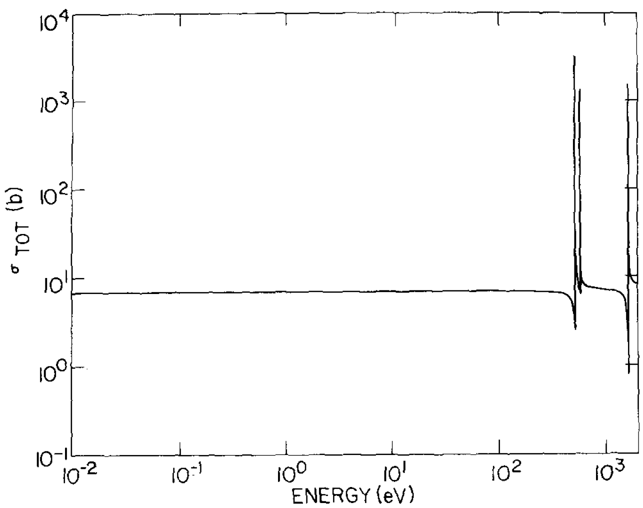

Figure 15. Total neutron cross section for ^{84}Kr (10^{-2} eV to 2 keV).

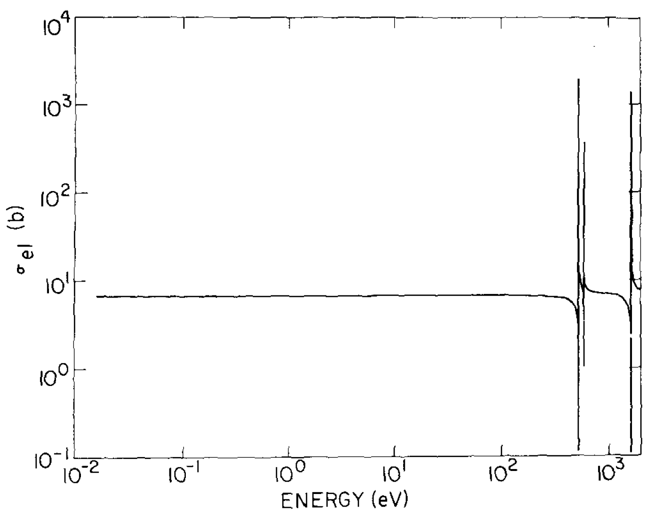

Figure 16. Elastic neutron cross section for ^{84}Kr (10^{-2} eV to 2 keV).

where

A = mass of nucleus

U = effective energy of excitation ($U = E_B - \Delta$)

E_B = binding energy of compound nucleus

Δ = $\delta(N) + \delta(p)$ the pairing energy

I = spin of target nucleus

a = single-particle state density parameter near the Fermi surface.

The relation between a and A are based on the analysis of Cook et al.[6] where

$$\frac{a}{A} = 0.009175 + 0.142$$

$S = S(N) + S(a)$ shell correction parameter

Eq. (1) produced the following radiation widths

Kr 78	Γ_γ = 266 meV
Kr 80	Γ_γ = 237 meV
Kr 82	Γ_γ = 236 meV
Kr 83	Γ_γ = 233 meV
Kr 84	Γ_γ = 226 meV
Kr 86	Γ_γ = 168 meV

A comparison of these widths with experimental data and calculations of Malecky et al.[5] are shown in Figure (1).

Krypton-78 (MAT 1181)

For Kr^{78} the experimental data in Table 1 yielded a value of $\sigma_{n\gamma}$(2200m) = 0.156b which is much lower than the value of 4.71 ± 0.68b[7].

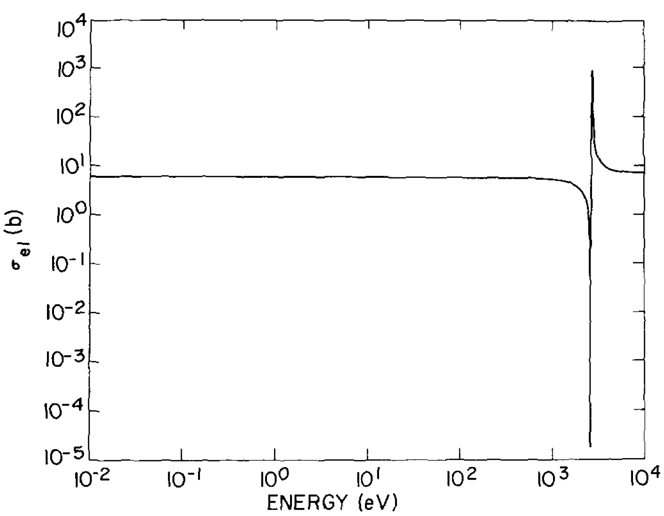

Figure 19. Elastic neutron cross section for ^{86}Kr (10^{-2} eV to 10 keV).

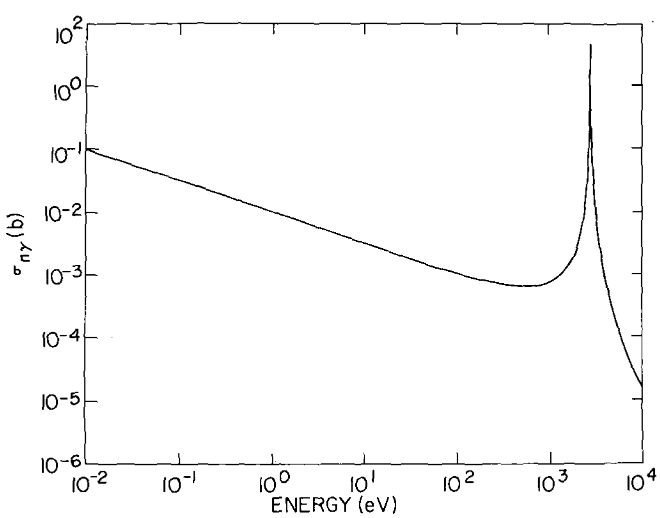

Figure 20. Capture neutron cross section for ^{86}Kr (10^{-2} eV to 10 keV).

Elastic Scattering

$$\sigma_{nn}^{\ell}(m) = (2\ell + 1)\, \frac{4\pi}{k_m^{\,2}} \sin^2 \phi_\ell$$

$$+ \frac{\pi}{k_m^{\,2}} \sum_J g_J \sum_{r=1}^{N_{res}(\ell,J)} \frac{\Gamma_{nr}^2 \cos 2\phi - 2\Gamma_{nr}\, (\Gamma_{\gamma r} + \Gamma_{fr}) \sin^2\phi_\ell}{(E - E_r{}')^2 + \left(\frac{\Gamma_r}{2}\right)^2}$$

$$+ \frac{2(E - E_r{}')\, \Gamma_{nr} \sin 2\phi_\ell}{(E - E_r{}')^2 + {\frac{\Gamma_r}{2}}^2} \qquad (1)$$

Capture

$$\sigma_{n\gamma}^{\ell}(m) = \frac{\pi}{k_m^{\,2}} \sum_J g_J \sum_{r=1}^{N_{res}(\ell,J)} \frac{\Gamma_{nr}\Gamma_{\gamma r}}{(E - E_r{}')^2 + \left(\frac{\Gamma_r}{2}\right)^2} \quad . \quad (2)$$

where m is the m^{th} isotope,

$N_{res}(\ell,J)$ are the number of resonances for a given ℓ and J,

$$\Gamma_{nr}(E) = \frac{P_\ell(E)\,\Gamma_{nr}(|E_r|)}{P_\ell(|E_r|)} \quad .$$

$$\Gamma_r = \Gamma_{nr}(E) + \Gamma_{\gamma r}$$

$$E_r{}' = E_r + \left(\frac{S_\ell(|E_r|) - S_\ell(E)}{2P_\ell(E_r|)}\right) \Gamma_{nr}(|E_r|) \qquad (E \text{ in eV}) \ ,$$

$$k_m = 2.196771 \times 10^{-3} \left(\frac{AWR}{AWR + 1.0}\right) \sqrt{E}(eV) \quad (barns)^{-1/2} \ ,$$

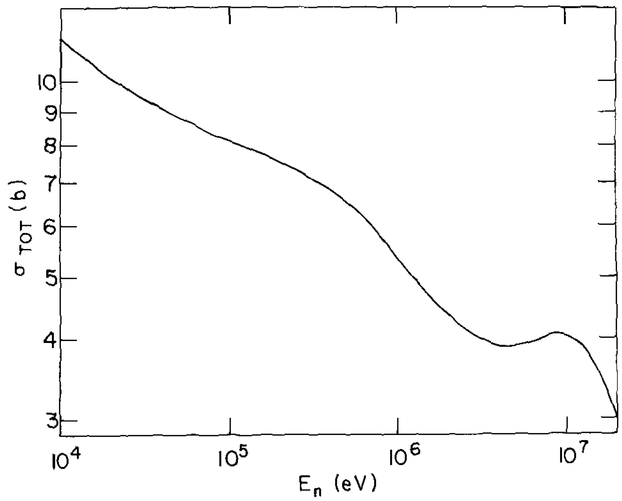

Figure 23. Total neutron cross section for ^{82}Kr (10 keV to 20 MeV).

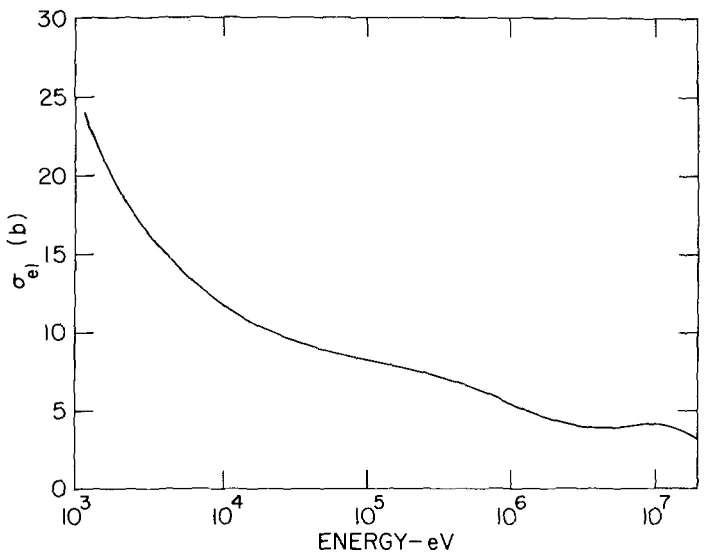

Figure 24. Total neutron cross section for ^{83}Kr (1.127 keV to 20 MeV).

Fig.		Page
37	Capture Neutron Cross Section for ^{82}Kr (10 keV to 20 MeV)	47
38	Capture Neutron Cross Section for ^{83}Kr (1.127 keV to 20 MeV)	47
39	Capture Neutron Cross Section for ^{84}Kr (2 keV to 20 MeV)	48
40	Capture Neutron Cross Section for ^{86}Kr (10 keV to 20 MeV)	48

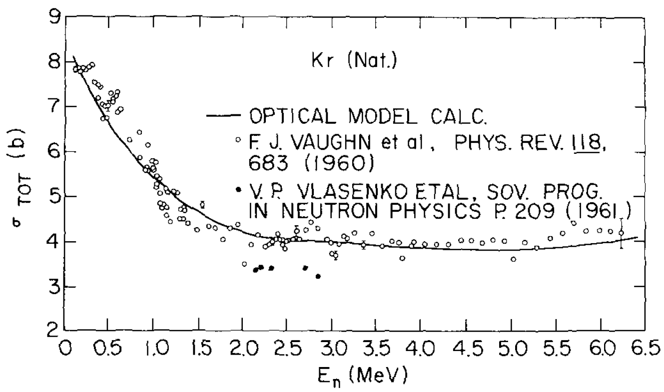

Figure 27. Optical model calc. for Kr (Nat.) (E $\leq$ 6.5 MeV).

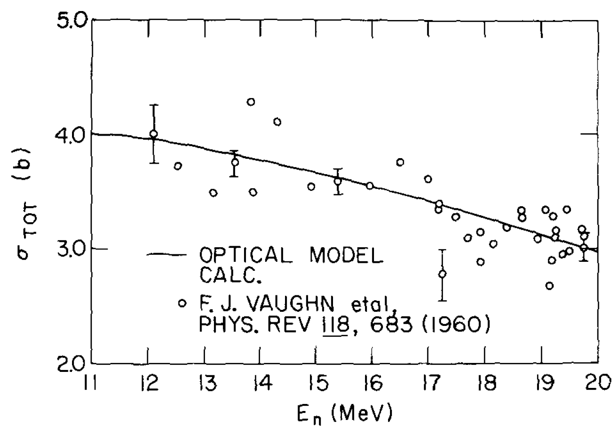

Figure 28. Optical model calc. for Kr (Nat.) (E = 11 to 20 MeV).

Fig.		Page
13	Elastic Neutron Cross Section for ^{83}Kr (10^{-2} eV to 1.127 keV)	35
14	Capture Neutron Cross Section for ^{83}Kr (10^{-2} eV to 1.127 keV)	35
15	Total Neutron Cross Section for ^{84}Kr (10^{-2} eV to 2 keV)	36
16	Elastic Neutron Cross Section for ^{84}Kr (10^{-2} to 2 keV)	36
17	Capture Neutron Cross Section for ^{84}Kr (10^{-2} eV to 2 keV)	37
18	Total Neutron Cross Section for ^{86}Kr (10^{-2} eV to 10 keV)	37
19	Elastic Neutron Cross Section for ^{86}Kr (10^{-2} eV to 10 keV)	38
20	Capture Neutron Cross Section for ^{86}Kr (10^{-2} eV to 10 keV)	38
21	Total Neutron Cross Section for ^{78}Kr (1 keV to 20 MeV)	39
22	Total Neutron Cross Section for ^{80}Kr (10 keV to 20 MeV)	39
23	Total Neutron Cross Section for ^{82}Kr (10 keV to 20 MeV)	40
24	Total Neutron Cross Section for ^{83}Kr (1.127 keV to 20 MeV)	40

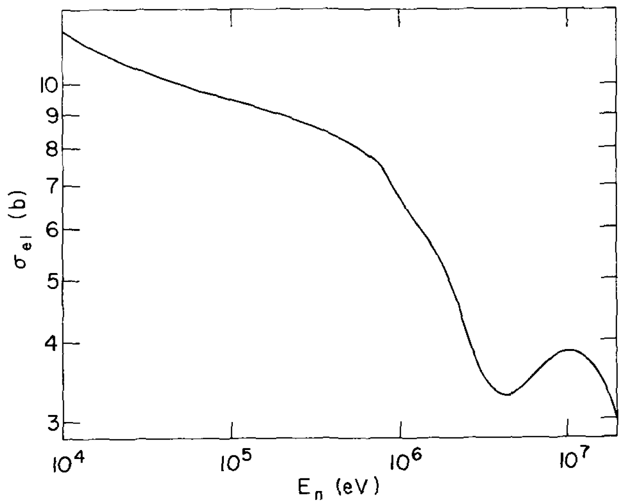

Figure 31. Elastic neutron cross section for ^{82}Kr (10 keV to 20 MeV).

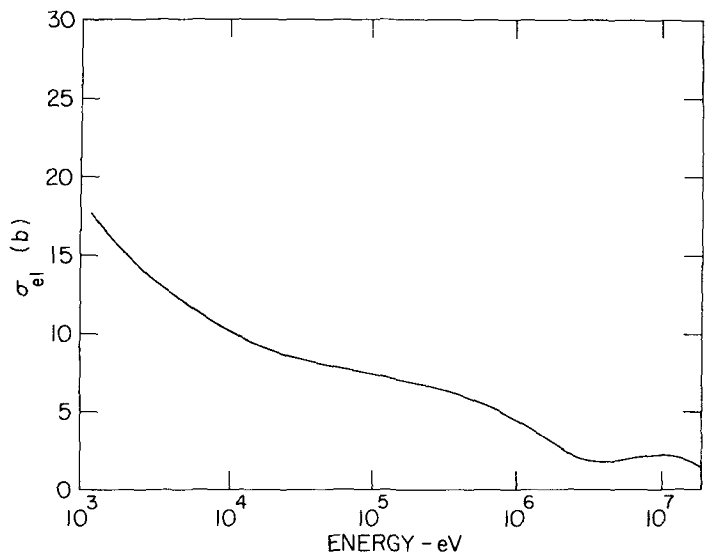

Figure 32. Elastic neutron cross section for ^{83}Kr (1.127 keV to 20 MeV).

List of Tables

Table No.		Page
1	Experimental Resonance Parameters	15
2	Adopted Resonance Parameters	16
3	Q Values for ^{78}Kr	17
4	Q Values for ^{80}Kr	18
5	Q Values for ^{82}Kr	19
6	Q Values for ^{83}Kr	20
7	Q Values for ^{84}Kr	21
8	Q Values for ^{86}Kr	22
9	Data for Statistical Model Calculations of ^{78}Kr	23
10	Data for Statistical Model Calculations of ^{80}Kr	23
11	Data for Statistical Model Calculations of ^{82}Kr	24
12	Data for Statistical Model Calculations of ^{83}Kr	25
13	Data for Statistical Model Calculations of ^{84}Kr	26
14	Data for Statistical Model Calculations of ^{86}Kr	27
15	Neutron Activation Cross Sections at 14.4 ± 0.3 MeV for Kr Isotopes	28

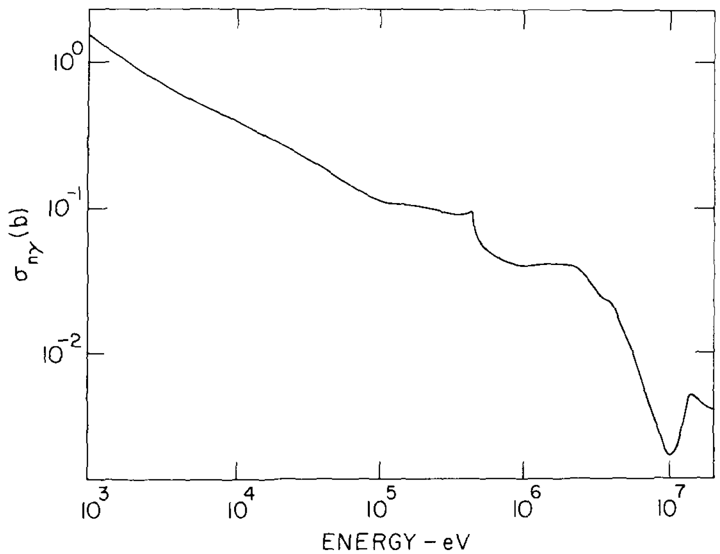

Figure 35. Capture neutron cross section for ^{78}Kr (1 keV to 20 MeV).

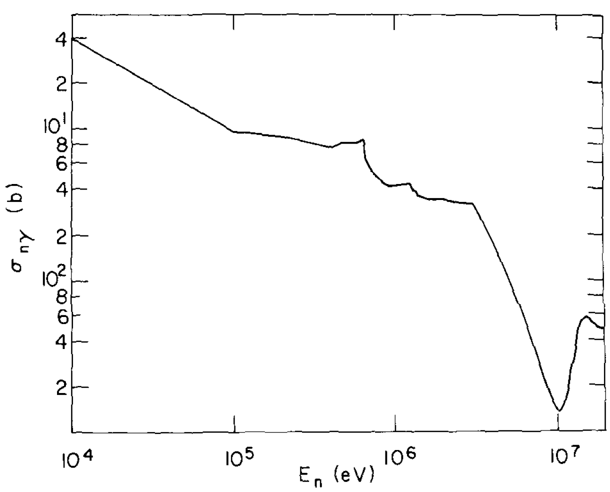

Figure 36. Capture neutron cross section for ^{80}Kr (10 keV to 20 MeV).

Printed in the United States of America
Available from
National Technical Information Service
U.S. Department of Commerce
5285 Port Royal Road
Springfield, VA 22161
Price: Domestic $5.50; Foreign $8.00;
Microfiche $2.25

March 1976 600 copies

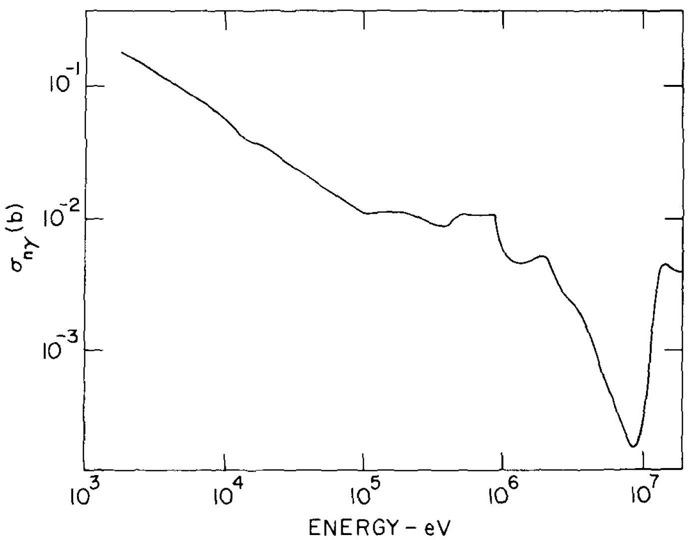

Figure 39. Capture neutron cross section for ^{84}Kr (2 keV to 20 MeV).

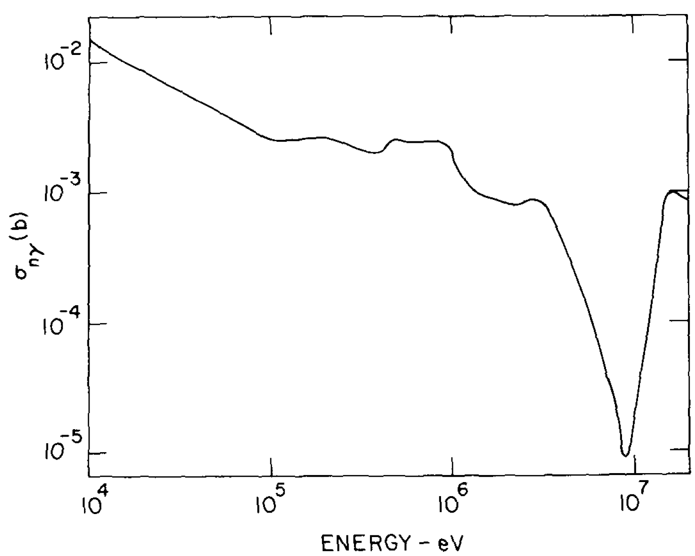

Figure 40. Capture neutron cross section for ^{86}Kr (10 keV to 20 MeV).

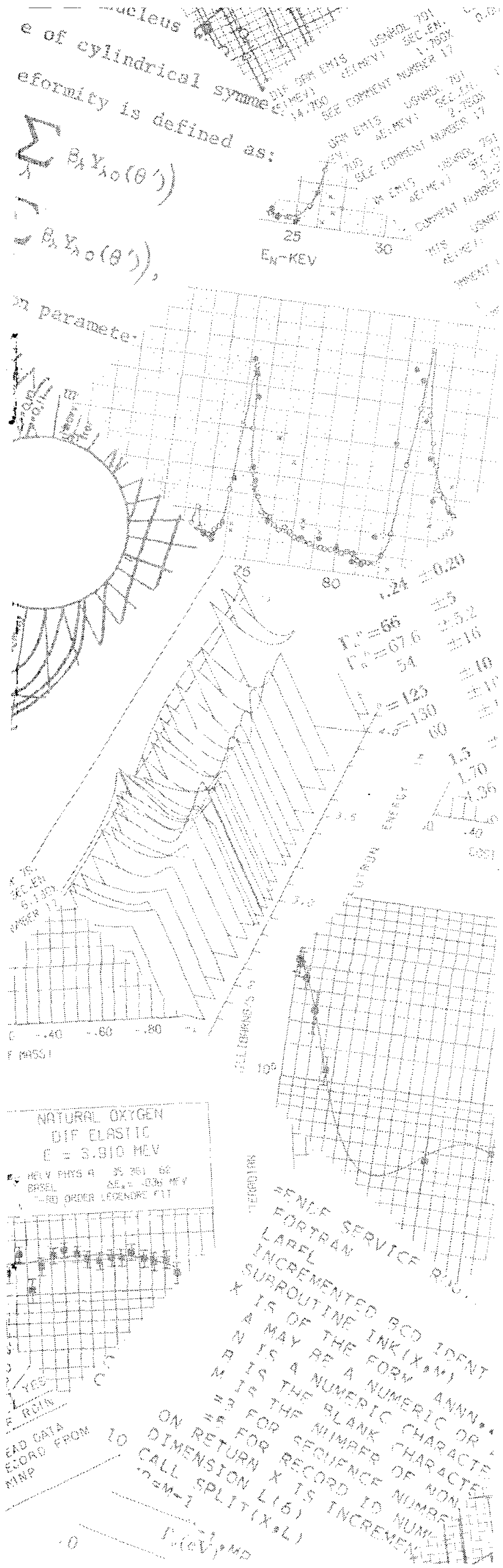

BNL-NCS-50503
(ENDF-232)

EVALUATION OF NEUTRON CROSS SECTIONS FOR THE KRYPTON ISOTOPES

A. PRINCE

August 1974

INFORMATION ANALYSIS CENTER REPORT

NATIONAL NEUTRON CROSS SECTION CENTER
BROOKHAVEN NATIONAL LABORATORY
UPTON, NEW YORK 11973